Changes of the occupied density of defect states of *a*-Si:H upon illumination

W. Graf, K. Leihkamm, M. Wolf, J. Ristein, and L. Ley
Institut für Technische Physik, Universität Erlangen-Nürnberg, D-91058 Erlangen, Germany
(Received 14 July 1995)

We study the light-induced transient changes of the near surface density of occupied states $g(E)$ of undoped and boron-doped *a*-Si:H with photomodulated total photoelectron yield spectroscopy. The data show an increase of $g(E)$ upon illumination between 0.35 eV above E_F and 0.7 eV below E_F (towards the valence band) and a decrease in the region of deep valence-band-tail states. The difference signal depends sublinearly on the laser intensity and reaches a maximum of $\Delta g \approx 10^{17}$ cm^{-3} eV^{-1} at a laser intensity of 30 mW cm^{-2} ($\lambda = 532$ nm). Time-resolved measurements reveal rise and decay times of the order of milliseconds. The experimental results are explained quantitatively by a recombination model. In the framework of this model, a range of deep defects around mid-gap energy are singly occupied and neutral at probe-light intensities. Additional illumination with a laser leads to double occupation of these defects and a decrease of the valence-band-tail occupation.

I. INTRODUCTION

a-Si:H has been a major candidate for optoelectronic devices such as thin-film solar cells and thin-film transistors. The defect structure is therefore of great interest. The Staebler-Wronski effect, i.e., the metastable increase of the defect density of states upon illumination has been analyzed extensively over the past decades.[1,2] In recent years one began to focus on transient processes. There have been a number of experiments that indicate that there are transient changes of the occupied defect density of states in *a*-Si:H upon electrical bias or light bias.[3–8] One of the experimental methods used in these studies is total photoelectron yield spectroscopy (TPEYS). TPEYS is particularly well-suited for the study of *a*-Si:H surfaces. The relaxed momentum conservation requirements and lack of conduction-band structure in *a*-Si:H allow the extraction of the occupied electronic density of states over nearly the entire band gap directly form the measured yield spectra. The large dynamic range (10^7:1 up to 10^{10}:1) and high-energy resolution ($\Delta E \leqslant 0.1$ eV) of this electron-emission spectroscopy are ideal for the study of the occupation of band-tail and defect states.[9]

Hirabayashi *et al.* first extended the method to a dual-beam experiment.[8] In addition to the probe light the sample is illuminated with a laser. They observed an increase in the occupied density of defect states $g(E)$ in undoped samples between E_F and 0.7 eV below the Fermi level upon light bias ($\hbar\omega = 1.9$ eV). Here the term "below E_F" refers to energy levels towards the valence band.

In Ref. 3 it was shown that these changes occur on the time scale of milliseconds. The analysis of the data was based on the assumption that the occupation of defect states is not disturbed significantly at probe light intensities. Then for negligible correlation energy, all states which are below the Fermi energy E_F by more than a few k_BT are fully occupied without laser bias and no increase due to reoccupation is possible upon additional laser illumination. Furthermore it was shown that even for a finite correlation energy the data cannot be explained if thermal occupation under probe light was assumed.

In Ref. 4 two microscopic mechanisms for a transient change of the defect density of states were discussed: weak bond–dangling bond conversion[2,10] or a slow energetic relaxation of the defect following a change in occupation of the defect.[11] Both models require time constants for the lattice relaxation in the range of milliseconds. Such long time constants are not generally accepted for *a*-Si:H.

In this paper we show that the assumption of thermal occupation of states under typical probe light intensities in a photoemission yield experiment is not valid. In fact, if this assumption is dropped, the experimental observation can be explained as a charging of the defect states upon additional illumination.

II. PHOTOMODULATED TOTAL PHOTOELECTRON YIELD SPECTROSCOPY

In conventional photoelectron spectroscopies such as ultraviolet photoelectron spectroscopy (UPS) or x-ray photoelectron spectroscopy (XPS), the energy distribution of electrons excited from the sample by monochromatic light is measured. In total photoelectron yield spectroscopy, all of the photoemitted electrons, regardless of their kinetic energy, are collected (total yield) and the energy of the incident light is varied ($4\text{ eV} \leqslant \hbar\omega \leqslant 6$ eV). The resulting total yield spectrum $Y(\omega)$ is defined as the number of electrons emitted from a solid into the vacuum per incident photon of energy $\hbar\omega$. For *a*-Si:H, the spectrum of ionization energies $S(\hbar\omega)$ can be obtained as follows:[12]

$$S(\hbar\omega) \propto [\hbar\omega]^4 \left[\frac{4Y(\hbar\omega)}{\hbar\omega} + \frac{d}{d\hbar\omega} Y(\hbar\omega) \right]. \tag{1}$$

The derivation of Eq. (1) is based on the three-step model of photoemission. The energy dependence of the average optical transition-matrix element $R(\omega)$ is approximated by the relation $R^2 \propto \hbar\omega^{-5}$. If one neglects the energy dependence of the matrix element Eq. (1) reduces to

$$S(\hbar\omega) \propto \frac{d}{d\hbar\omega} Y(\hbar\omega). \tag{2}$$

Yield spectroscopy is a surface-sensitive method with a probe depth of the order of 10 nm for photon energies of 4–6 eV. Thus $S(\hbar\omega)$ gives information about *both* the density of surface states and the density of near-surface states. For zero correlation energy the spectrum of ionization energies $S(\hbar\omega)$ may be identified with the density of occupied states $g(E)$ according to $g(-E)=S(\hbar\omega)$ if the energy is set to zero at the vacuum level.

The ionization energies of singly and doubly occupied states are different in the case of a finite correlation energy. The relation between $g(E)$ and the one-electron density of states $D^1(E)$ (strictly speaking the one-electron density of ionization energies) may be written in the form

$$g(E)=f^0(E)D^1(E)+2f^-(E-U_{\rm opt})D^1(E-U_{\rm opt}). \quad (3)$$

Here $U_{\rm opt}$ is the difference between the ionization energy of a singly occupied state and a doubly occupied state, and $f^0(E)$ and $f^-(E)$ are the occupation probabilities for single and double occupation of a state at energy E, respectively.[13] In the absence of lattice relaxation $U_{\rm opt}$ is identical to the Coulomb energy difference U_C for singly and doubly occupied states. If there is a significant lattice relaxation, no simple relation between $D^1(E)$and $g(E)$ exists.[14] For convenience, in what follows we refer to $g(E)$ as the occupied density of states in all cases.

If the generation rate in a-Si:H due to the probe light is low enough the occupation of the defect density of states should still be in thermal equilibrium. Thus, neglecting a finite correlation energy it should be possible to determine the density of states from Eq. (3) by simply dividing $g(E)$ by the Fermi-Dirac distribution function. This approach has been applied in Ref. 15 for n-type a-Si:H to determine the density of conduction-band-tail states.

A major extension of the method is photomodulated total yield photoelectron spectroscopy (PM-TPEYS).[4,7,8] PM-TPEYS is a dual-beam experiment. The pump light is used to modify the properties of the sample without producing photoelectrons. The occupied density of states $g(E)$ and its changes due to the pump light are examined with the probe light beam that produces photoelectrons. Typical probe light energies in our experiment are 3–6 eV and intensities of the order of 10 μW/cm^2.

The photomodulation of the yield spectra was measured using a frequency doubled Nd:YAG (yttrium-aluminum-garnet) laser (532 nm, $I_{\rm max}=30$ mW cm^{-2}) as bias light source or a HeNe laser (633 nm, 180 mW/cm^2). Details have been published elsewhere.[3]

In what follows the index L refers to laser illumination and the index Y to probe light conditions. For both, probe light ($\hbar\omega_Y$) and pump light ($\hbar\omega_L$) the relation $\hbar\omega \geq E_G$ is valid.

Here E_G is the optical gap of a-Si:H. Thus the major effect of both probe and pump light on the sample is the generation of electron-hole pairs. The generation rate G for these pairs depends on the light intensity and the absorption coefficient of the sample.[2] For probe light intensities $G=10^{16}$–10^{18} cm^{-3} s^{-1} in our experiment, depending on the energy of the photons. Generation rates of $G_L=10^{21}$–10^{22} cm^{-3} s^{-1} are achieved under pump light illumination.

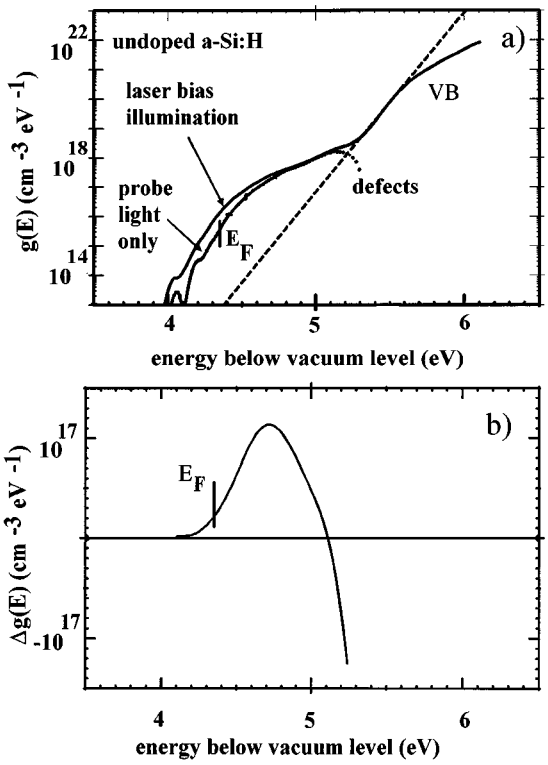

FIG. 1. Occupied density of states $g(E)$ of a-Si:H under probe light excitation (a) and upon additional laser illumination and the difference $\Delta g(E)$ of the two spectra (b).

Undoped and boron-doped a-Si:H films were deposited by the rf glow discharge decomposition of silane and diboran on stainless steel substrates. The deposition temperature was 250 °C, the rf power 5 watts, electrode area 25 cm^2, electrode distance 2 cm, gas flow 4 sccm, deposition pressure 0.3 mbar, deposition time 1 h. The samples were transferred under UHV conditions directly after the deposition to a UHV analysis chamber where the work function, transient and stationary surface photo voltage of the samples were determined with a Kelvin probe[16] and the occupied density of states by total photoelectron yield spectroscopy.

III. RESULTS

A. Steady-state measurements

Figure 1 shows two typical occupied density of states spectra $g(E)$ at probe light intensity ($G=G_Y$) and upon laser illumination ($G=G_Y+G_L$). The spectra have been normalized to 10^{22} cm^{-3} eV^{-1} at 6.2 eV following the procedure given in Ref. 12. The Fermi energy was measured with a Kelvin probe. It is positioned at 4.35 eV below the vacuum level. The integrated near-surface density of defect states amounts to 3×10^{17} cm^{-3}. Upon illumination with the laser beam there is a transient increase of $g(E)$ between 4.0 and 5.1 eV below the vacuum level (Fig. 1). The maximum enhancement at 4.75 eV corresponds to $\sim10^{17}$ states cm^{-3} eV^{-1} and the integrated number of photoinduced states with ionization energies between 4.3 and 5 eV amounts to

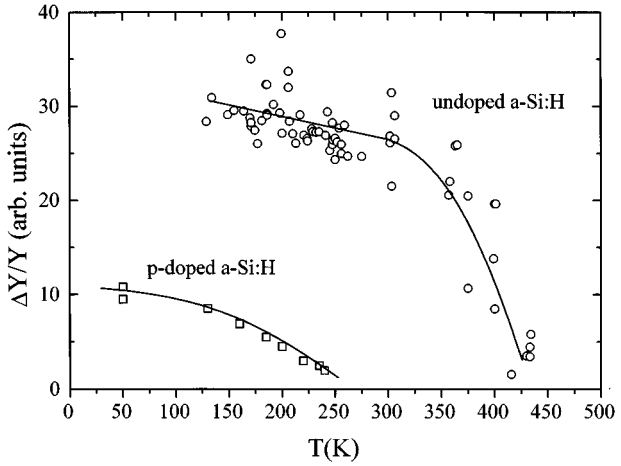

FIG. 2. Temperature dependence of the modulation $\Delta Y/Y$ at $\hbar\omega$=4.8 eV, i.e., the increase of the integrated spectrum of ionization energies integrated up to that photon energy upon band-gap illumination for undoped a-Si:H (several samples) and boron-doped a-Si:H (100 ppm). The solid lines are guides to the eye. Details are given in the text.

3.5×10^{16} cm^{-3}, i.e., ~10% of the total number of deep defects. For Boron-doped samples (100 ppm) a similar increase of $g(E)$ is observed.

To determine the temperature dependence of the laser-induced signal we have measured the steady-state increase of the yield signal $\Delta Y=Y(G_Y+G_L)-Y(G_Y)$, at a probe light energy of 4.8 eV. According to Eq. (2) this is essentially the increase in the integrated occupied density of states $g(E)$ from the vacuum level to a binding energy of 4.8 eV if in addition to the probe light the sample is illuminated by the laser. The result is shown in Fig. 2. For the undoped sample the signal decreases very weakly between 120 and 350 K. Above that temperature, however, the signal drops to zero within ~100 K.[4] For boron-doped samples ΔY increases significantly with decreasing temperature in the whole temperature range examined.

The relative enhancement $\Delta Y/Y$ of the photoinduced signal at a binding energy of 4.8 eV as a function of the generation rate is shown in Fig. 3. For the p-doped samples we

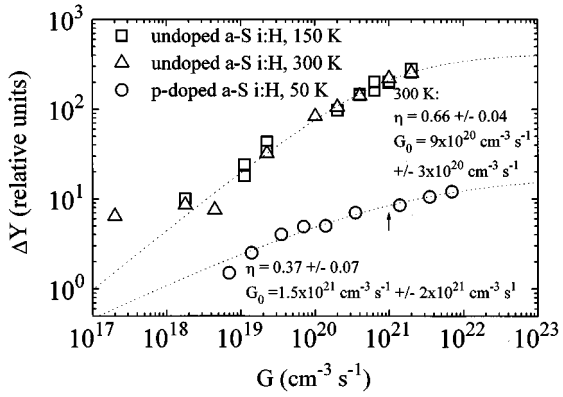

FIG. 3. Light-induced relative yield enhancement $\Delta Y/Y$ as a function of the generation rate G of electron-hole pairs for undoped a-Si:H (150 and 300 K) and boron-doped a-Si:H (100 ppm). The dashed lines are fits according to $\Delta Y(G)\propto 1/[1+(G_0/G)^{\eta}]$.

use for statistical reasons the low-temperature data (50 K) for this comparison. The increase of ΔY can be described by a power-law behavior (G^a) for low generation rates. A phenomenological expression for $\Delta Y(G)$ can be derived if one assumes that there is a light-induced conversion of reservoir of states N^0 with a rate constant r_1 and the annihilation of $\Delta N(t)$ with a rate constant r_2:[4]

$$\frac{d}{dt}Y\propto\frac{d}{dt}\Delta N(t)=r_1[N^0-\Delta N(t)]-r_2\Delta N(t). \qquad (4)$$

In the microscopic models discussed below it will be shown that N^0 is either the number of singly occupied defects that is converted into doubly occupied defects ΔN, or the number of defects in a configuration D^0 that change their ionization energies due to slow lattice relaxation or the number of weak bonds that is converted into defect states ΔN (i.e., precursors of the Staebler-Wronski effect).

r_1 is assumed to depend on the light intensity as

$$r_1=r_2\left[\frac{G}{G_0}\right]^{\eta}.$$

The steady-state solution of Eq. (4) is then

$$\Delta Y(G)\propto\frac{1}{1+\left[\frac{G_0}{G}\right]^{\eta}}. \qquad (5)$$

Good agreement with the intensity dependence in Fig. 3 is obtained for $G_0\approx9\times10^{20}$ cm^{-3} s^{-1} and $\eta=0.66\pm0.1$ in the case of undoped samples and $G_0\geqslant1.5\times10^{21}$ cm^{-3} s^{-1}, $\eta=0.37\pm0.1$. In time-resolved experiments, which will be discussed in the next section, one expects the rise to depend on r_1+r_2 and the decay time constant to be $\tau_d=r_2^{-1}$.

B. Transients

The transient response of the light-induced yield ΔY at 4.8 eV and maximum pump light intensity ($G_L=2\times10^{21}$ cm^{-3} s^{-1}) is shown in Fig. 4. The data were obtained using a multichannel analyzer in combination with a light beam chopper. Up to 10 000 cycles were necessary to obtain sufficient accuracy. Since the decay transient is not fully relaxed when the next cycle starts the transients in Fig. 4(a) start at $\Delta Y\neq0$. The return to the dark level is shown in Fig. 4(b). It is about a factor of 10 slower than the rise time. Both rise and decay transients slow down with lower temperature. The rise transients can be fitted with a single exponential with time constants τ_r as indicated in Fig. 4(a). In contrast to the model of Eq. (4) the longer decay transients cannot be described by a single exponential decay function with time constant τ_d. We use a superposition of exponential decays with distribution function $P(\tau_d)$ for the time constants:

$$Y(t)\propto\int_0^{\infty}P(\tau_d)e^{-t/\tau_d}d\tau_d. \qquad (6)$$

Often in solid-state physics decay time constants are connected by an exponential relationship with a microscopic control parameter (such as the tunneling distance between localized states or the thermal activation energy for the rate limiting step). Even without specifying the microscopic

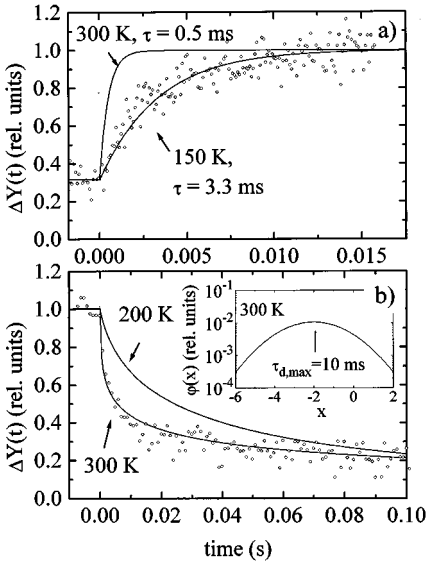

FIG. 4. (a) Rise of the laser-induced yield signal at 4.8 eV for 150 K (data and fit) and 300 K (fit only). The modulation period was 0.1 s. The decay transient has not reached its minimum value yet when the rise transient begins. The minimum value thus had to be determined separately. (b) Decay transient at 300 K. The fit consists of a superposition of exponential decay transients according to the time constant distribution shown in the insert. $\tau_{d,\max}$ is used to characterize the decay.

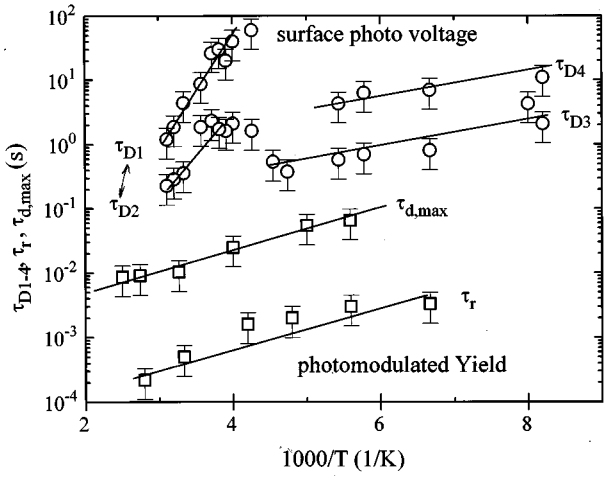

FIG. 5. Comparison between the initial slope decay time constants of the surface photovoltage transients extracted from Fig. 6 and the time constants for rise and decay of ΔY upon illumination from Fig. 4. As can be seen, the decay of the surface photovoltage transients is more than one order of magnitude slower than the decay of the change in ΔY, and exhibits a different temperature dependence.

mechanism for the transient yield changes it is therefore reasonable to transfer the distribution function $P(\tau_d)$ to a logarithmic scale. With the substitution $x=\ln(\tau_d/1s)$ the corresponding distribution function $\varphi(x)$ is then related to $P(\tau_d)$ by

$$\varphi(x)=P(10^x s)\ln(10)10^x s \tag{7}$$

with the inverse relationship

$$P(\tau_d)=\frac{\varphi[\log_{10}[\tau_d/s]]}{\ln[10]\tau_d}. \tag{8}$$

We use as an ansatz a Gaussian distribution for $\varphi(x)$:

$$\varphi(x)=\frac{1}{\sqrt{2\pi\sigma}}e^{[x-x_0]^2/[2\sigma^2]}. \tag{9}$$

The parameter τ_d in Eq. (4) has thus to be related to the average value x_0 of the logarithmic time constant x. For the fits in Fig. 4(b) $\sigma=1.5$, $\tau_{d,\max}=10^{x_0}s=0.01$ s at 300 K and $\sigma=0.7$, and $\tau_{d,\max}=0.04$ s at 200 K. The insert shows the decay time distribution for 300 K. Both rise and decay transients slow down with decreasing temperature. The time constants as a function of temperature are shown in the lower part of Fig. 5.

IV. DISCUSSION

Our analysis of the data is based on Eq. (3) which results from the three-step model of photoemission. In the limit of zero correlation energy Eq. (3) results in $g(E)=2f(E)D(E)$. A change in $g(E)$ upon laser illumination can in general either be due to a change in the occupation function $f(E)$ or a change in the one-electron density of states $D(E)$ or both.

A change in $f(E)$ can be due to (1) a change in the occupation *without* a displacement of electrons relative to holes in space, i.e., without a change in space charge density; (2) a change in the occupation including a displacement of the charge in space.

If a change in $f(E)$ is accompanied by a displacement of net charge in space, a change in band bending is to be observed. We thus performed photomodulated time-resolved Kelvin probe experiments. The aim was to find out whether the change in $g(E)$ observed in PM-TPEYS is due to a change in surface band bending upon illumination.

What can be the origin of a change in the density of states $D(E)$? Two microscopic mechanisms have been examined: (3) The precursor of the Staebler-Wronski effect, i.e., transient opening of a weak bond in an exciting state creating two dangling-bond defects for a limited time; (4) defect relaxation, i.e., the evolution of its total energy after change of its occupation. In what follows the four models will be discussed.

A. Surface photovoltage

Hydrogenated amorphous silicon exhibits surface band bending.[8,17,18] The band bending changes upon illumination and results in a surface photovoltage (SPV). Since photoelectron yield spectroscopy is a surface-sensitive technique the analysis of the influence of a change of surface band bending, which is usually accompanied by a change in the occupation of surface states and surface near defects upon illumination is very important for the photomodulated yield spectra. We have measured the change of the contact potential difference (CPD) of our samples upon illumination with a Kelvin probe. In undoped a-Si:H the bands "bend down" upon illumination relative to their dark position by 100 mV at laser intensities comparable to those used in the photo-

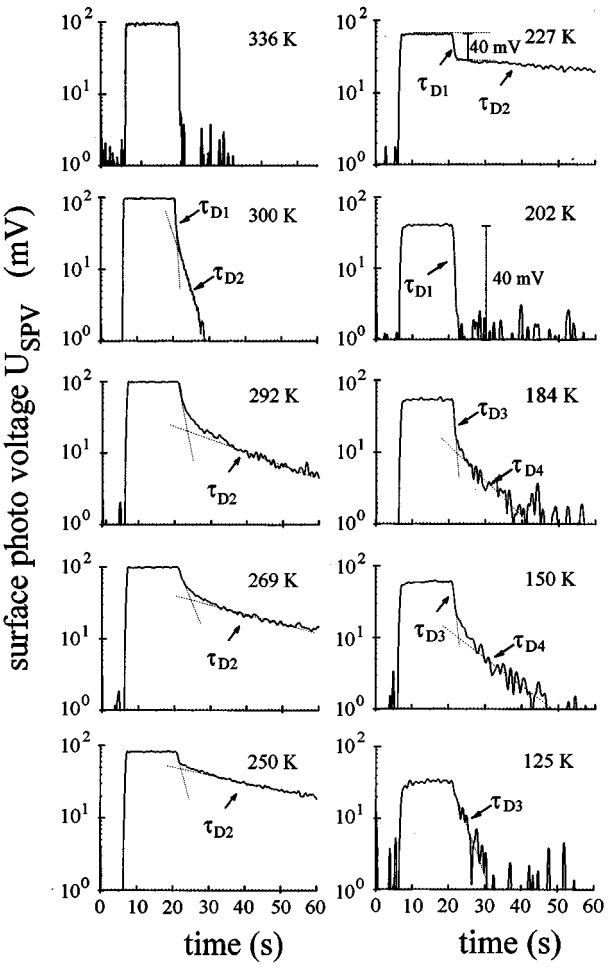

FIG. 6. Rise and decay transients of the surface photovoltage upon laser illumination (532 nm, 50 mW/cm^{-2}) for various temperatures.

modulated yield experiments. In 100 ppm boron-doped samples the bands bend *up* by 100–200 mV. Thus the effect of surface band bending on the occupation should be of opposite sign. However, the transient changes observed are of the same sign for undoped and boron-doped samples. Furthermore, we have measured the decay transients of the surface photovoltage as a function of temperature with a resolution of 0.1 s. The result is shown for various temperatures in Fig. 6. The rise of the signal cannot be resolved experimentally. The decay transient consists of a fast and a slow component labeled τ_{D1} (τ_{D3}) and τ_{D2} (τ_{D4}), depending on the temperature regime. Details of the experiment will be presented elsewhere. The time constants extracted from the data are shown in the upper part of Fig. 5.

Also shown in Fig. 5 are the time constants τ_r and $\tau_{d,\max}$ of ΔY for rise and decay determined as shown in Fig. 4. The decay times for ΔY differ from those of the surface photovoltage by 1–2 orders of magnitude. We thus infer that the change in $g(E)$ is a local process in contrast to the occurrence of a SPV which requires charge separation. Therefore we can assume that the changes in $g(E)$ are not due to a change in surface band bending.

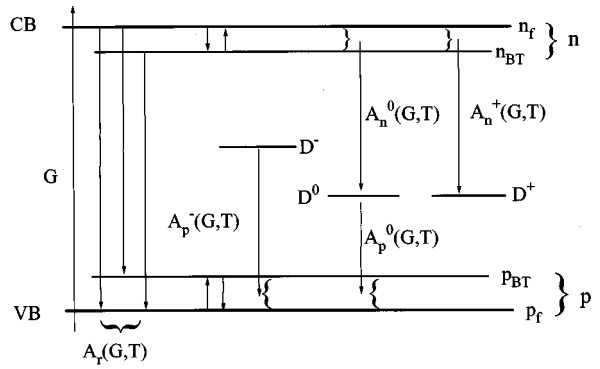

FIG. 7. Generation and recombination transitions of our model. The transition coefficients $A_i^j(G,T)$ take into account the fact that only free carriers recombine. Details in text.

B. Rate-equation model for the occupation of defects

In this section we consider changes in the occupation of defects and band-tail states under strong illumination. There have been a number of publications on the occupation of defects in *a*-Si:H upon illumination.[2,6,19] Major simplifications are possible in the determination of the occupation functions if thermal excitation from defects can be neglected. Our approach is based on Ref. 2. The integral quantities considered in our model are n_f, density of free electrons; n_{BT}, density of electrons in the conduction band tail; N^-, density of negatively charged dangling bonds; N^0, density of neutral dangling bonds; N^+, density of positively charged dangling bonds; p_{BT}, density of holes in the valence band tail; p_f, density of free holes.

The relationship between the density of electrons and holes and the population of the dangling-bond states under steady-state illumination is governed by the transitions shown in Fig. 7. Generation of carriers is restricted to the excitation of electrons from the valence band into the conduction band. Thermalization to the band edges is assumed to be fast. Furthermore, we assume that recombination occurs only via transitions from extended to extended or extended to localized states. Thermal excitation from deep defects is neglected. This is a valid assumption if the occupation of the defect states is dominated by recombination of photogenerated electrons and holes. In order to show that this assumption is justified to describe our experiment not only for pump light intensities but also for probe light conditions we apply the Rose criterion.[20] According to Rose, thermal emission rates from defects e_n, e_p can be neglected if they are small compared to capture rates R of electrons or holes. The capture rate of an electron into a neutral defect is usually written in the form

$$R_n^0 = n_f v_{\mathrm{th}} \sigma_n^0. \tag{10}$$

Here n_f is the concentration of electrons in extended states, v_{th} is the thermal velocity of the carriers, and σ_n^0 is the capture cross section of a free electron into a neutral dangling bond. Similar relations hold for the other transitions. The thermal excitation rate of an electron from a negatively charged defect $e_n^-(E)$ is given by

$$v_n^-(E) = \nu_0 \, e^{-(E_{\mathrm{CBME}}-E)/k_B T}. \tag{11}$$

Here E_{CBME} is the conduction-band mobility edge. Using $v_{\mathrm{th}}=10^7$ cm/s, $\sigma_n^0 \approx 10^{-15}$ cm^2, $n_f > 10^{10}$ cm^{-3}, $\nu_0=10^{12}$ s^{-1} at and below room temperature the relation $e_n^-(E) \leqslant R_n^0$ holds for states situated by more than 0.6 eV below the conduction-band mobility edge. Similar relations are valid for neutral and positively charged defect states. As will be shown below, free carrier densities of the order of 10^{10} cm^{-3} can be obtained even for probe light intensities in a photoelectron yield experiment. Considering a mobility gap of about 2.0 eV for *a*-Si:H and symmetrical conditions for electrons and holes for our rough estimate, the occupation of a range of defects 0.5 eV around mid gap should be determined exclusively by the balance of electrons and hole capture. For these defects thermal excitation of carriers can be neglected and the model outlined below holds. The energy of such a defect does not enter into the model and the occupation functions for the dangling bonds do not obey Fermi statistics but instead $n^0=N^0/N_r$ and the $n^-=N^-/N_r$ are independent of E.

The rate equation model defined by Fig. 7 can be simplified if one defines the fractions of free carriers in extended states to the total amount of excited carriers in extended and band-tail states f_n and f_p by

$$f_n=\frac{n_f}{n_f+n_{\mathrm{BT}}}, \quad f_p=\frac{p_f}{p_f+p_{\mathrm{BT}}}. \tag{12}$$

Using these ratios we define effective transition coefficients A_n^i and A_p^i by

$$A_n^i=n f_n v_{\mathrm{th}} \sigma_n^i, \quad i=0,+, \quad A_p^i=p f_p v_{\mathrm{th}} \sigma_p^i, \quad i=0,-, \tag{13}$$

which get an additional implicit temperature dependence via f_n and f_p. Here $n=n_f+n_{\mathrm{BT}}$, $p=p_f+p_{\mathrm{BT}}$. With the above definitions the rate equations under steady-state conditions are as follows (see also Fig. 7):

$$0=\frac{d}{dt}n=G-A_n^0(G,T)nN^0-A_n^+(G,T)nN^+-A_t(G,T)np, \tag{14}$$

$$0=\frac{d}{dt}N^-=A_n^0(G,T)nN^0-A_p^-(G,T)pN^-, \tag{15}$$

$$0=\frac{d}{dt}N^0=A_n^+(G,T)nN^+ +A_p^-(G,T)pN^- -A_n^0(G,T)nN^0 - A_p^0(G,T)pN^0, \tag{16}$$

$$0=\frac{d}{dt}N^+=A_p^0(G,T)pN^0-A_n^+(G,T)nN^+, \tag{17}$$

$$0=\frac{d}{dt}p=G-A_p^0(G,T)pN^0-A_p^-(G,T)pN^--A_r(G,T)np. \tag{18}$$

The transition coefficients are given by

$$A_n^0(G,T)=[v_{\mathrm{th}}(T)\sigma_n^0 f_n(G,T)], \qquad A_n^+(G,T)=[v_{\mathrm{th}}(T)\sigma_n^+ f_n(G,T)], \tag{19}$$

$$A_p^0(G,T)=[v_{\mathrm{th}}(T)\sigma_p^0 f_p(G,T)], \qquad A_p^-(G,T)=[v_{\mathrm{th}}(T)\sigma_p^- f_p(G,T)], \tag{20}$$

and

$$A_r(G,T)=f_n v_{\mathrm{th}}\sigma^{\mathrm{BT}}[1-f_p]+f_p v_{\mathrm{th}}\sigma^f f_n + f_p v_{p,\mathrm{th}}\sigma^{\mathrm{BT}}[1-f_n]. \tag{21}$$

σ^f and σ^{BT} denote the capture cross sections for the transition from extended to extended and extended to band-tail states, assumed to be identical for electrons and holes, respectively. The coefficient A_r for bimolecular recombination consists of the recombination of free electrons with free holes, free electrons with holes in the valence-band tail, and free holes with electrons in the conduction-band tail.

The replacement of n_f and p_f by $f_n n$ and $f_p p$ in the above equations is particularly useful if it is possible to show that f_n and f_p are approximately independent of the generation rate. In order to determine f_n for electrons, we apply the Boltzmann approximation to obtain an approximate value for the ratio n_f/n_{BT}. The value does not depend on the position of the quasi-Fermi-level for trapped electrons as long as $k_B T > E_{\mathrm{CBT}}$, where E_{CBT} is the characteristic energy of the slope of the conduction-band tail.[21] For lower temperatures f_n has to be determined numerically. Our analysis gives $f_n \approx 0.1$ at room temperature for a conduction-band-tail slope of $E_{\mathrm{CBT}}=25$ meV and a density of states at the mobility edge of $N_{\mathrm{CBME}}=10^{21}$ cm^{-3} eV^{-1}. The value is independent of the generation rate at 300 K within a factor of 3. At higher temperatures it is independent of G, at lower temperatures it exhibits a strong dependence on the generation rate. In addition, f_n decreases rapidly with decreasing temperature below 300 K. f_p exhibits a stronger dependence on the position of the quasi-Fermi level for free holes (and thus on the generation rate). For $E_{\mathrm{VBT}}=50$ meV and $N_{\mathrm{VBME}}=10^{21}$ cm^{-3} eV^{-1}, $f_p=10^{-4}$ (10^{-5}) for $E_{F_p}-E_{\mathrm{VBME}}=0.4$ eV (0.5 eV) at room temperature.

We point out here that the strong asymmetry between f_n and f_p in *a*-Si:H is due to the different slopes of the valence- and conduction-band tails.

Our theoretical estimate for f_n and f_p may be compared to $f_{n,\mathrm{drift}}=\mu_{0n}/\mu_{Dn}$ and $f_{p,\mathrm{drift}}=\mu_{0p}/\mu_{Dp}$, i.e., the ratio of the free carrier mobility μ_0 and the time-of-flight drift mobility μ_D for electrons and holes. According to Ref. 19 typical values are $f_{n,\mathrm{drift}} \approx 0.07$, $f_{p,\mathrm{drift}} \approx 0.003$. Since $f_p \ll f_n$, Eq. (21) can be simplified: the major contribution is due to the recombination of free electrons with holes in the valence-band tail.

The final boundary conditions that determine the solution are the equation for the conservation of the total number of dangling bonds and the conservation of charge. The former can be written in the form

$$N_r=N^+ +N^0+N^-. \tag{22}$$

The equation for the conservation of charge can be written in the form

$$\frac{Q}{eN_r}=\frac{q}{e}=[n^+-n^-]+\frac{p-n}{N_r}. \tag{23}$$

TABLE I. Capture cross sections and transition coefficients assuming $f_n=0.1$ and $f_p=10^{-4}$ ($f_p=10^{-5}$); scattering cross sections into defects have been taken from Ref. 22. $v_{th}=10^7$ cm/s.

Transition	σ_i^j (cm^2)	$A_i^j=f_i\sigma_i^j v_{th}$ (cm^3 s^{-1})
$D^0+p\rightarrow D^+$	8×10^{-15}	$A_p^0=8\times10^{-13}$ (8×10^{-12})
$D^-+p\rightarrow D^0$	2×10^{-14}	$A_p^-=2\times10^{-12}$ (2×10^{-11})
$D^0+n\rightarrow D^{-1}$	2.7×10^{-15}	$A_n^0=2.7\times10^{-9}$
$D^++n\rightarrow D^0$	1.3×10^{-14}	$A_n^+=1.3\times10^{-8}$
$n+p\rightarrow/$	5×10^{-16}	$A_r=5\times10^{-10}$

Here Q is the charge per unit volume. Q does not include the charged donors or acceptors. Their occupation is assumed to be constant. Furthermore $n^+=N^+/N_r$, $n^0=N^0/N_r$, and $n^-=N^-/N_r$. q/e is positive for p-doped samples, negative for n-doped samples, and zero for undoped samples.

To summarize, we have formally reduced the more general rate equation model defined by Fig. 7 to the one discussed by Ref. 2. Our model makes a distinction between free carriers and carriers in band-tail states. Due to the asymmetry of valence- and conduction-band-tail slope in a-Si:H and thus the fact that $f_p \ll f_n$, we have been able to simplify the equations. As a result, there is a strong asymmetry between the effective transition coefficients of electrons and holes, in contrast to Ref. 2. In addition, due to the generation rate dependence of f_n (at low temperatures) and f_p below about 600 K the transition coefficients do also depend on G. It is this dependence which will finally explain the redistribution of electrons seen in the photomodulated photoyield experiment.

From the above equations it follows that

$$\frac{q}{e}\mp 2\left[\frac{1}{4}\{1-n^0\}^2-\frac{\{n^0\}^2}{\beta}\right]^{1/2}=\frac{1}{N_r}[p-n], \tag{24}$$

with

$$n=\frac{N_r}{2A_r}[A_p^0n^0+A_p^-n^-]\left[\left(1+\frac{4A_rG}{[N_r]^2[A_p^0n^0+A_p^-n^-][A_n^0n^0+A_n^+n^+]}\right)^{1/2}-1\right], \tag{25}$$

and

$$p=\frac{N_r}{2A_r}[A_n^0n^0+A_n^+n^+]\left[\left(1+\frac{4A_rG}{[N_r]^2[A_p^0n^0+A_p^-n^-][A_n^0n^0+A_n^+n^+]}\right)^{1/2}-1\right], \tag{26}$$

$$n^+=\frac{1}{2}[1-n^0]\pm\left[\frac{1}{4}\{1-n^0\}^2-\frac{\{n^0\}^2}{\beta}\right]^{1/2}, \tag{27}$$

$$n^-=\frac{1}{2}[1-n^0]\mp\left[\frac{1}{4}\{1-n^0\}^2-\frac{\{n^0\}^2}{\beta}\right]^{1/2}, \tag{28}$$

β is defined by

$$\beta:=\frac{N^0N^0}{N^+N^-}=\frac{A_p^-A_n^+}{A_p^0A_n^0}. \tag{29}$$

As has been pointed out by Ref. 8, β fully determines the occupation of the dangling-bond states in undoped material at low generation rates provided thermal rates can be neglected. Although the transition coefficients depend on the generation rate G in our approach, β is independent of G since f_n and f_p cancel in the definition of β.

The upper sign in Eqs. (27) and(28) refers to a positive average charge in the defects, the lower one to negatively charged defects. n^0 is given by Eq. (24), with G to be the only parameter. The roots n^0 have to be determined numerically in most cases. In the following we discuss the solution of Eq. (24) for $q/e=0$ (undoped a-Si:H) and $q/e=1$ (p-doped a-Si:H).

1. Undoped a-Si:H

In undoped a-Si:H the average number of electrons per defect is approximately 1, i.e., the average charge of a defect is zero, $q/e=0$. It has been shown in Ref. 2, that at low generation rate the above equations reduce to

$$n^0\approx n^0_{max}=\frac{\beta^{1/2}}{[2+\beta^{1/2}]},\quad n^+\approx n^-\approx\frac{1}{[2+\beta^{1/2}]}, \tag{30}$$

$$n\approx\frac{G}{N_r}\frac{1}{[A_n^0n^0+A_n^+n^+}},\quad p\approx\frac{G}{N_r}\frac{1}{[A_p^0n^0+A_p^-n^-}}. \tag{31}$$

The reason for $n^+=n^-$ is that $n,p\ll N_rn^+$, N_rn^-. As one can see, n^0 and n^- are independent of g and T in this regime. Thus in this regime the TPEYS spectra of undoped a-Si:H should be independent of probe light intensity and temperature.

The transition between low and high generation rates has to be determined numerically. We use the bulk capture cross sections given by Ref. 22, a velocity of the free carriers $v_{th}=10^7$ cm/s and the ratios $f_n=0.1$, $f_p=10^{-4}$ ($f_p=10^{-5}$). The resulting transition coefficients are given in Table I. The near-surface density of defect states was obtained experimentally to be $N_r=10^{17}$ cm^{-3}. In Fig. 8 the result of our numerical solution for $f_p=10^{-4}$ and $f_p=10^{-5}$ is displayed. n

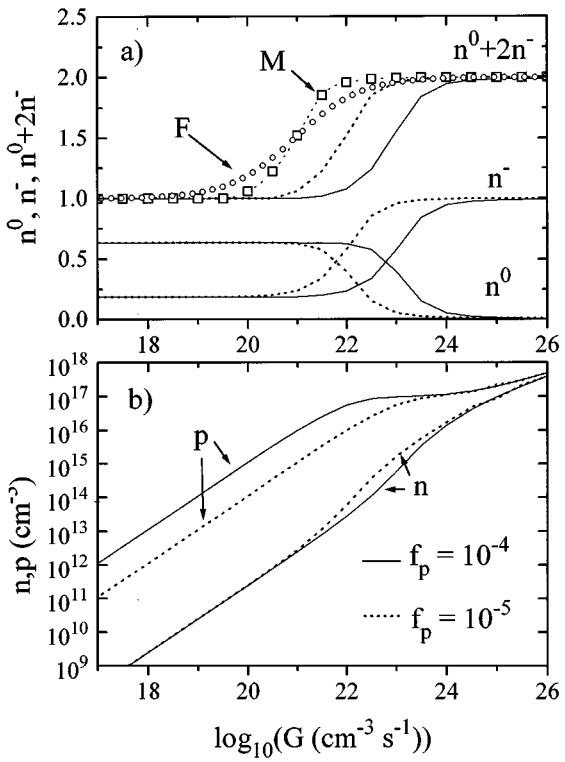

FIG. 8. n^0, n^-, n, and p as a function of G for undoped a-Si:H. Constant effective transition coefficients are assumed. The solid lines correspond to $f_p=10^{-5}$, the dotted lines to $f_p=10^{-4}$, $f_n=0.1$, defect density $N_r=10^{17}$ cm^{-3} in both cases. Also shown is the fit from Fig. 3 [F in Fig. 6(a)] for $\eta=0.66$, $G_0=9\times10^{20}$ cm^{-3} s^{-1}. The line labeled M corresponds to $N_r=3\times10^{16}$ cm^{-3} and $f_p=10^{-5}$.

and p are the electron and hole densities, the fraction of singly occupied defects is labeled n^0, that of doubly occupied defects n^-, and the average charge per defect n^0+2n^-. n^+ can be obtained from the relation $n^-+n^0+n^+=1$.

At low generation rates, n and p increase linearly with the generation rate G. In this generation rate range n^0 and n^- are determined by β and do not depend on G significantly. Since $f_p \ll f_n$, more holes than electrons are trapped in band-tail states due to the asymmetry in the effective recombination coefficients. The difference in charge, n-p, gives the density of electrons trapped in defects. Since those are, however, much more than n and p, they are still neutral on the average.

If the generation rate is increased, p approaches the density of defects N_r. Then for reasons of charge neutrality a significant charging of the defects takes place.

At sufficiently high generation rates all defects are finally doubly occupied. In this range $n \approx p \propto G^{0.5}$.

In analogy with Fig. 3, the transition between low and high generation rates may be characterized by a generation rate G_0, where the increase in the average defect occupation n^0+2n^- reaches 50% of the maximum value. As can be seen in Fig. 8, a reduction of f_p by one order of magnitude shifts the transition region by one order of magnitude to lower generation rates. In our model G_0 depends on the generation rate: $G_0 \propto f_p^{-1} N_r^2$.

To compare the model with the relative increase of the yield $\Delta Y/Y$ (Fig. 3) we point out that n^0+2n^--1 is proportional to the integrated increase of occupied density of defect states. The relative increase of curve F in Fig. 8(a) shows the normalized fit for undoped a-Si:H in Fig. 3 on a linear scale. The observed transition occurs at lower G than predicted by the model. G_0 can only be reproduced if we either assume $f_p=10^{-6}$ for $N_r=10^{17}$ cm^{-3} or $f_p=10^{-5}$ for $N_r=3\times10^{16}$ cm^{-3}. $f_p=10^{-6}$ is not compatible with the spectral shape of our data. Since the experimentally observed defect density is $N_r \geqslant 10^{+17}$ cm^{-3}, $N_r=3\times10^{+16}$ cm^{-3} is only consistent with our data if part of the experimentally observed defect density does not contribute to the increase observed. This may be due to the fact that our model neglects thermal rates. Since only defect states between the quasi-Fermi levels for electrons and holes are optically occupied, N_r may be smaller than the total number of defects.

Another discrepancy between our model for constant f_p and the experimental data is the slope of the transition region. A fit of Eq. (5) to n^0+2n^- in Fig. 3 gives $\eta \geqslant 1$. The experimental value, however, is $\eta=0.66\pm0.1$, as shown in Fig. 3. This discrepancy can be explained by the fact that the dependence of f_p on the generation rate has been neglected in our numerical calculation. Qualitatively, f_p increases at higher generation rates. Thus the transition region is broadened. This results in a reduction of η. A quantitative comparison can only be performed in a self-consistent numerical simulation beyond our semianalytical approach.

We next turn to the discussion of the spectral dependence of the photoinduced yield signal. In Fig. 9 the experimental data of Fig. 1 are compared with the result of our simulation. In the upper part of Fig. 9 the experimental spectrum $g(E)$ is shown for probe light intensities (G_Y) and for laser illumination (G_L). The theoretical spectra $g(G_Y)$ and $g(G_L)$ have been obtained according to Eq. (3). As mentioned above, N_r is smaller than the experimental value for the integrated defect density of states, most likely due to the fact that defect states outside the region between the quasi-Fermi levels are still in thermal equilibrium. This hypothesis is supported by the fact that the maximum of the increase occurs at an ionization energy of 4.8 eV, i.e., approximately at mid gap. A Gaussian shape for the one-electron density of defect states $D^1(E)$ within the quasi-Fermi levels is therefore assumed with integral value $N_r=3\times10^{+16}$ cm^{-3}. The occupation follows from our rate-equation model. $n^0=0.64$, $n^-=0.18$ for G_Y and $n^0=0.15$, $n^-=0.84$ for G_L. An optical correlation energy $U_{\rm opt}=0$ gives an upper limit of 1 for the relative increase of $g(E)$ upon illumination. Since our data show $g(G_L)/g(G_Y)\approx4$ at 4.25 eV (see insert in Fig. 9) $U_{\rm opt}$ must be greater than 0. We assume $U_{\rm opt}=0.1$ eV. However, our data is not very sensitive to $U_{\rm opt}$.

The dotted line in Fig. 9(a) with a maximum at 5.4 eV gives the change in the density of trapped holes. The area is equal to the increase of the charge in the defect states. In Fig. 9(b) the difference spectra are shown. As can be seen, the experimental data can be fitted quite well in the energy range from 4 to 5 eV. For statistical reasons no information is obtained about the shape of the hole distribution.

Finally, within our approach, the time constants can be estimated as follows: to charge 10^{17} defects per cm^3 at a generation rate of $G=10^{21}$ cm^{-3} s^{-1} takes at least 10^{-4} s. This value is close to what we observe for τ_r at room temperature. Recombination of the excess carriers in the defect

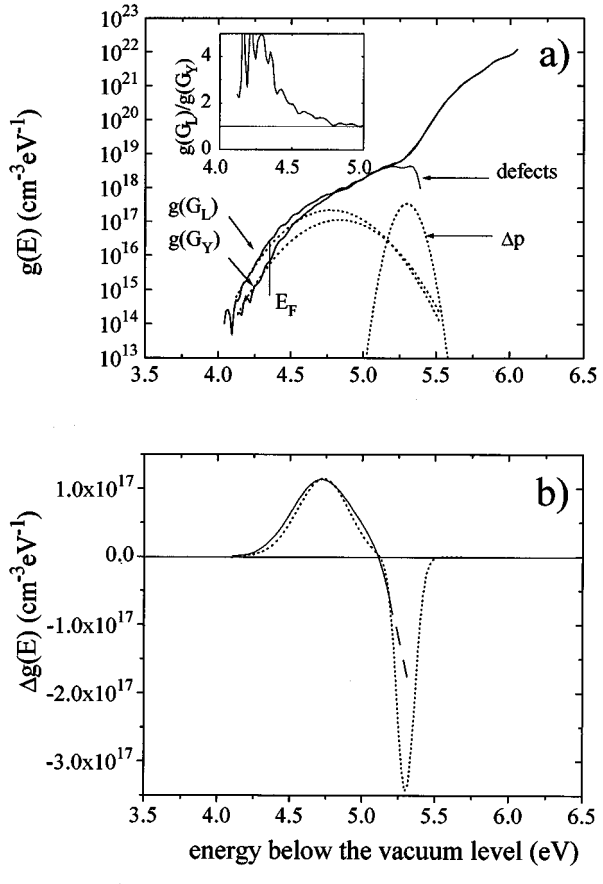

FIG. 9. Spectral changes in the pseudogap of a-Si:H upon additional illumination according to our model. The solid lines correspond to the experimental data, the broken lines are theoretical fits. Details in text.

states after the pump light has been switched off, on the other hand, occurs at probe light intensities and will thus take much longer. However, a more complicated numerical approach is required to compare the time constants quantitatively.

2. Boron-doped a-Si:H

We restrict our discussion to $q/e=1$. This is a good approximation to describe boron-doped samples with a doping concentration of $B_2H_6 \geqslant 100$ ppm. In this case all defects are positively charged in the dark. In Fig. 10 the numerical solution of Eq. (24) for $q/e=1$ is shown. The transition coefficients used were the same as those for undoped a-Si:H (Table I), the defect density is higher than that in undoped material. In the computation we took $N_r=10^{18}$ cm^{-3}. In contrast to Fig. 8(a) we choose a logarithmic scale for the plot of the fractions n^0 and n^-. The dependence of n^0 and p on the generation rate differs considerably from undoped material. Both density functions increase proportional to $G^{0.5}$ at low generation rates. At a sufficiently high generation rate all defect states will again be negatively charged. The same saturation values as in undoped material are obtained.

In order to obtain an analytical expression for $N^0(G)$ at low generation rates we use the approximation given by Eq. (31) which also holds for the case of doping. Equation (24) for the conservation of the total charge is now reduced to

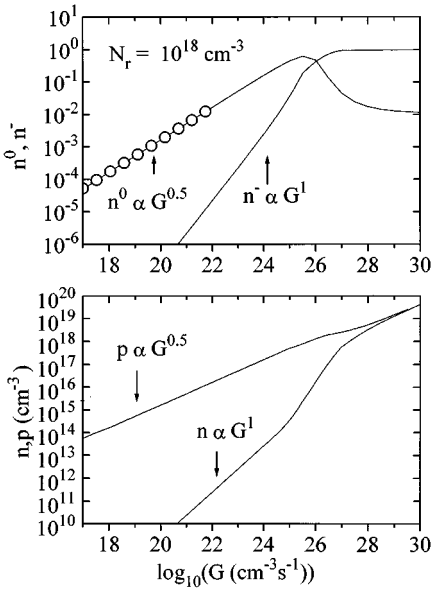

FIG. 10. Carrier densities and defect occupation in p-type a-Si:H as a function of the generation rate. $N_r=10^{18}$ cm^{-3}. The open circles are based on Eq. (34) and confirm the validity of our approximation.

$$1-2\left[\frac{1}{4}\{1-n^0\}^2-\frac{[n^0]^2}{\beta}\right]^{1/2}=\frac{G}{[N_r]^2}\left[\frac{1}{[A_p^0 n^0+A_p^- n^-]}-\frac{1}{[A_n^0 n^0+A_n^+ n^+]}\right]. \quad (32)$$

For p-type material $n^+\approx 1 \gg n^0 \gg n^-$. Furthermore, since the conduction-band tail is much steeper than the valence-band tail, $f_p \ll f_n$ and thus $A_p^0, A_p^- \ll A_n^0, A_n^+$. Equation (32) reduces to

$$1-[1-2n^0]^{1/2}=\frac{G}{[N_r]^2}\left[\frac{1}{[A_p^0 n^0]}\right]. \quad (33)$$

Since $n^0 \ll 1$, the square root on the left-hand side can be expanded to give

$$N^0(G,T)=n^0 N_r=\frac{G^{0.5}}{[A_p^0(G,T)]^{0.5}}. \quad (34)$$

Equation (34) shows that the density of singly occupied defects does only depend on the generation rate and the effective capture coefficient of holes into D^0 states. For a constant transition coefficient A_p^0, N^0 is thus proportional to $G^{0.5}$. The second feature of Eq. (34) is that the total number of electrons in defects does not depend on the absolute number of defect states.

We make use of these results and give a quantitative explanation for the observation in Ref. 11. It was found there that $g(E)$ in boron-doped samples ($B_2H_6=100$ ppm) depends on the temperature (Fig. 11). Note that in these experiments samples were only illuminated by the UV probe light of the photoyield experiment. According to Eq. (34) this can only be due to the temperature dependence of $A_p^0(G,T)$, since

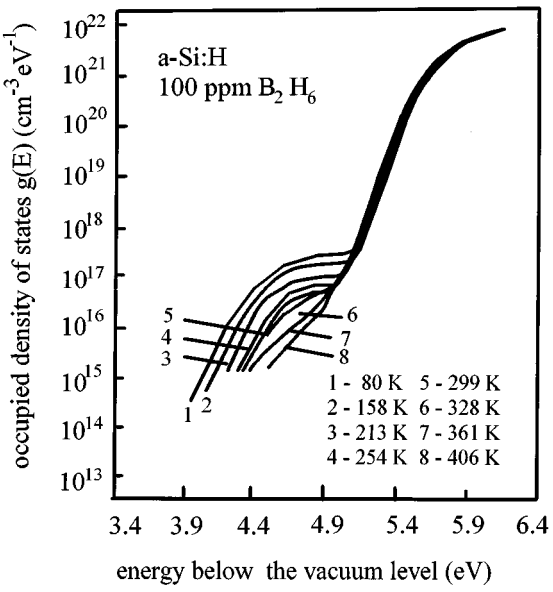

FIG. 11. Temperature dependence of the occupied density of states of boron-doped a-Si:H according to Ref. 7. As the temperature is reduced, the number of trapped carriers increases.

$G=G_Y$ was kept constant. In our model the temperature dependence of $A_p^0(G,T)$ is due to the fact that $f_p \equiv p_f/(p_f+p_{\mathrm{BT}})$ depends on the temperature [Eq. (20)]. If we assume that the occupation of the band tail can be described by a quasi-Fermi function with a quasi-Fermi energy independent of T, a numerical analysis gives a reduction of f_p of 3–4 orders of magnitude within the temperature range considered. This strong temperature dependence is reduced by the fact that the total number of holes increases with lower temperature, thus shifting the quasi-Fermi energy towards E_{VBME}. As a result a change over about two orders of magnitude is expected theoretically.

Typical probe light intensities in a yield experiment are of the order of $G=10^{18}$ cm^{-3} s^{-1} at 250 nm. In Fig. 12

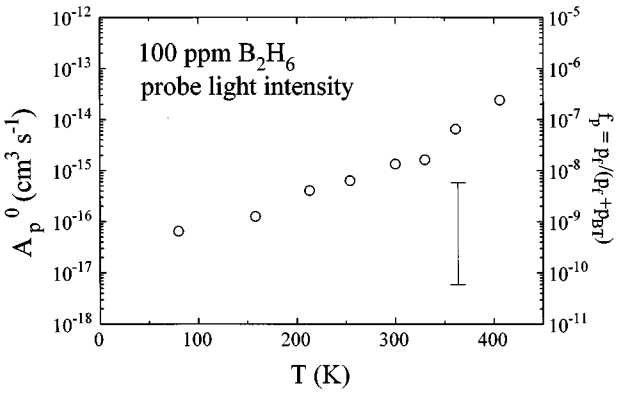

FIG. 12. Temperature dependence of the effective transition coefficient A_p^0 at probe light intensities ($G\approx 10^{18}$ cm^{-3} s^{-1}, the uncertainty in G is responsible for the error bar) calculated from the data of Ref. 7. On the right scale the ratio f_p calculated from $A_p^0=f_p v_{\mathrm{th}}\sigma_p^0$ is displayed assuming $v_{\mathrm{th}}=10^7$ cm/s and $\sigma_p^0=8\times10^{-15}$ cm^2.

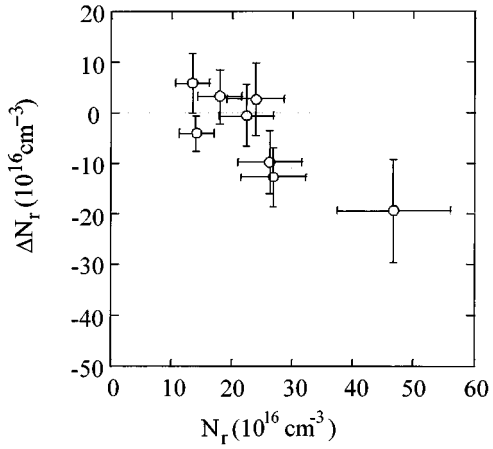

FIG. 13. Metastable changes of the integrated change of the occupied density of defect states of a-Si:H $g(E)$ after 12 h of illumination with white light (AM 3). Above an initial defect density of about 2×10^{17} cm^{-3} a decrease is observed upon white light illumination.

$A_p^0(G,T)$ as obtained from the spectra of Ref. 7 and Eq. (34) is plotted as a function of temperature. The axis on the right-hand side gives the corresponding ratio f_p assuming $v_{\mathrm{th}}=10^7$ m/s and $\sigma_p^0=8\times10^{-15}$ cm^{-2}. The temperature dependence can be seen quite clearly. It changes over more than 2 orders of magnitude between 200 and 400 K, in accordance with the theoretical estimate.

Thus the simple rate-equation model does in fact explain all the features exhibited by a photomodulated photoelectron yield experiment. For completeness in what follows we briefly discuss further microscopic effects that have been suggested as an explanation to our experiment. It cannot be fully excluded that they give an *additional* contribution to the experimental finding.

C. Precursor of the Staebler-Wronski effect

In addition to a charging of the defect states upon laser illumination, there may be a change of the defect density of states itself. This mechanism has been proposed as an explanation to our experiment on undoped a-Si:H in Ref. 3.

The most prominent changes of the defect density of states of a-Si:H are the Staebler-Wronski effect[1] (SWE) and light-induced annealing[22–25] (LIA). Since these changes are metastable, not transient, we should observe only a precursor of both in our experiment.

In order to compare the transient changes in $g(E)$ with metastable changes of the defect density, we performed degradation experiments and illuminated our samples with white light (Xe lamp, 300 mW/cm^2) for 12 h. Depending on the initial defect density of states, which was achieved by thermal annealing at various temperatures, we found a slight increase of the integrated density of *near-surface* defect states for an initial defect density $N_r \leq 2\times10^{17}$ cm^{-3} and a decrease above that value (Fig. 13). The initial near-surface defect density corresponding to the point of crossover is comparable to the saturation value of light-induced bulk defects under comparable illumination.[24] The spectral changes

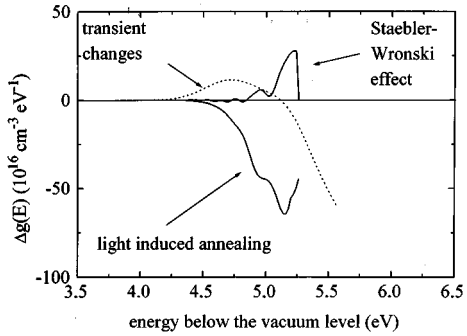

FIG. 14. Comparison between the experimentally determined change of the defect density of states according to metastable light-induced defect generation, metastable light-induced annealing, and transient changes in a photomodulation experiment. The experimental error for the metastable changes is 30% of the decrease (LIA).

for maximum increase and maximum decrease are shown in Fig. 14. They are compared to the transient change of the defect density from Fig. 1. Although the characteristic features of the weak-bond–dangling-bond conversion (i.e., increase in the region of deep defects, decrease in the region of deep tail states) can be found in all three spectra, the spectral shape of the transient and metastable changes differ considerably. It is therefore unlikely that the transient changes of $g(E)$ we observed in the photoyield experiment are due to transient weak-bond–dangling-bond conversion as a precursor of the SWE.

D. Defect relaxation

A second change of the defect density of states is currently discussed in the literature. Based on the work of Cohen *et al.*,[11] Han *et al.*,[5] and Branz *et al.*[14] argue that light bias effects observed in CPM measurements may be interpreted as a shift of D^0 states towards the conduction band upon carrier capture. This mechanism is based on the assumption that the ionization energy of an electron out of a defect does not only depend on the defect's occupation but also on the configuration of the surrounding network via electron-phonon coupling. Thus ionization of an electron from a D^0 state requires, for example, less energy if the arrangement of the surrounding atomic network corresponds to the relaxed configuration of a positively charged defect D^+ than to the appropriate D^0 equilibrium configuration. Usually, it is expected that lattice relaxation after recharging occurs so fast that defects can never be observed in configurations different from equilibrium. Cohen *et al.*, however, argue that atomic rearrangements on a large scale might be involved in amorphous semiconductors and thus relaxation times up to milliseconds could result.[26–29]

In Ref. 4 we outlined an approach of how to describe our experiment within the assumptions of a defect relaxation model. The approach is based on a proposal in Ref. 14. The optical excitation energies of an electron in a defect are assumed to depend on charge state and configuration. A capture of a hole by a D^0 defect, for example, could lead to the following ''reaction '' chain:

$$D^0(Q^0)+p^+\rightarrow D^+(Q^0) \xrightarrow{\text{fast relaxation}} D^+(Q^+), \qquad (35)$$

$$D^+(Q^+)+e^-\rightarrow D^0(Q^+) \xrightarrow{\text{slow relaxation}} D^0(Q^0). \qquad (36)$$

The observations in parentheses in Eqs. (35) and (36) indicate the configuration of the corresponding local defects. The system might then be caught in the photoyield experiment somewhere along the slow relaxation step depending on the ''feed rate'' $D^0+p^+\rightarrow D^+$, i.e., the light intensity. This results in a light-dependent shift of the D^0 defect band which is measured in TPEYS towards lower ionization energy. In general, one further has to take into account the relaxation of D^- states. We performed a Monte Carlo simulation to simulate both the processes and were able to reproduce the basic features of the experiment. Relaxation time constants in the range of milliseconds were required to fit the data. The results will be presented elsewhere. Besides the fact that lattice relaxation constants are beyond our current understanding of the material, the effect would only be a correction to the changes observed in undoped a-Si:H.

V. CONCLUSION

Experimental results of light-induced transient changes of the ionization-energy spectrum of the near-surface region of undoped and boron-doped a-Si:H upon above-band-gap illumination have been presented. These changes are not due to surface band bending, which exhibits significantly different time constants.

Our extension of the rate-equation model of Ref. 2 quantitatively explains all the features of the experiment. According to this model, the average occupation of a subset of dangling bonds between two quasi-Fermi levels is unity for probe light intensities ($G<10^{18}$ cm^{-3} s^{-1}) independent of the defect energy. Upon pump light intensities charging of the defects takes place due to different slopes of the valence-band tail and the conduction-band tail that is seen as an additional electron emission intensity below E_F in the yield spectrum.

Additional effects such as defect relaxation with time constants in the range of 1 ms as currently discussed in the literature could in principle be superimposed on the charging effect. Our numerical and analytical analysis, which we plan to publish, reveals that upon certain assumptions changes of the spectrum due to defect relaxation exhibit similar qualitative and quantitative features as reoccupation and thus cannot be excluded as an explanation. Defect relaxation, however, is not required to describe our experimental results.

For p-type material we have shown that defect occupation depends much more on the generation rate G as in undoped samples. In the limit of sufficiently low generation rates G we derived an analytical expression for the concentration of singly occupied defects N^0. It is given by $N^0=[G/A_p^0(G,T)]^{0.5}$, where $A_p^0(G,T)$ is the capture probability coefficient for holes by a neutral defect. This expression does in fact describe quantitatively the results given in Ref. 7 and explains the lower exponent in the intensity dependence compared to undoped samples.

Finally, our analysis is in accordance with recent LESR measurements on nonequilibrium occupancy of tail states and defects in undoped a-Si:H.[30] The authors performed a

numerical simulation on the occupation of defect states including the detailed distribution of defects according to the defect pool model. Significant charging of the defects at high generation rates and a high concentration of trapped holes in the valence-band tail are found.

ACKNOWLEDGMENT

This work was supported by the Deutsche Forschungsgemeinschaft under Project No. LE 634/3-2. The authors wish to thank J. D. Cohen and H. Branz for valuable discussions.

[1] D. L. Staebler and C. R. Wronski, Appl. Phys. Lett. **31**, 292 (1977).
[2] M. Stutzmann, W. B. Jackson, and C. C. Tsai, Phys. Rev. B **32**, 23 (1985).
[3] W. Graf, K. Leihkamm, J. Ristein, and L. Ley, in *Amorphous Silicon Technology–1993*, edited by E. A. Schiff, M. J. Thompson, A. Madan, and K. Tanaka, MRS Symposia Proceedings Vol. 297 (Materials Research Society, Pittsburgh, 1993).
[4] W. Graf, M. Wolf, K. Leihkamm, J. Ristein, and L. Ley, J. Non-Cryst. Solids **164–166**, 15 (1993).
[5] D. Han and Y. Xiao, in *Amorphous Silicon Technology–1993* (Ref. 3).
[6] J. Z. Liu, G. Lewen, J. P. Conde, and P. Roca i Caborracas, in *Amorphous Silicon Technology–1993* (Ref. 3).
[7] D. Cohen *et al.*, in *Physics of Semiconductors, Twentieth International Conference*, edited by E. M. Anastassakis and J. D. Joannopoulos (World Scientific, Singapore, 1990), Vol. 3, pp. 2071–2074.
[8] I. Hirabayashi, K. Winer, and L. Ley, J. Non-Cryst. Solids **97&98**, 87 (1987).
[9] J. Schäfer, J. Ristein, and L. Ley, Rev. Sci. Instrum. **64**, 653 (1993).
[10] M. Stutzmann, Philos. Mag. B **60**, 531 (1989).
[11] J. D. Cohen, T. M. Leen, and R. J. Rasmussen, Phys. Rev. Lett. **69**, 3358 (1992).
[12] K. Winer, I. Hirabayashi, and L. Ley, Phys. Rev. B **38**, 7680 (1988).
[13] D. Adler and E. J. Yoffa, Phys. Rev. Lett. **36**, 1198 (1976).
[14] Howard M. Branz and Eric A. Schiff, Phys. Rev. B **48**, 8667 (1993).
[15] A. Aljishi, J. D. Cohen, S. Jin, and L. Ley, Phys. Rev. Lett. **64**, 2811 (1990).
[16] Lord Kelvin, Philos. Mag. **46**, 82 (1898).
[17] B. Goldstein and D. J. Szostak, Surf. Sci. **99**, 325 (1980).
[18] M. Foller, W. Beyer, J. Herion, and H. Wagner, Surf. Sci. **178**, 47 (1986).
[19] R. Street, *Hydrogenated Amorphous Silicon* (Cambridge University Press, Cambridge, 1991).
[20] Albert Roses, RCA Rev. **12**, 362 (1951).
[21] K. Hattori, H. Okamoto, and Y. Hamakawa, Phys. Rev. B **45**, 1126 (1992).
[22] R. A. Street, Philos. Mag. B **49**, L15 (1984).
[23] H. Gleskova, P. A. Morin, and S. Wagner, Appl. Phys. Lett. **62**, 2063 (1993).
[24] C. F. O. Graeff and M. Stutzmann, Appl. Phys. Lett. **62**, 3001 (1993).
[25] Jong-Hwan Yoon, Phys. Rev. B **51**, 10 221 (1995).
[26] R. A. Street and N. F. Mott, Phys. Rev. Lett. **35**, 1293 (1975).
[27] M. Kastner, D. Adler, and H. Fritzsche, Phys. Rev. Lett. **37**, 1504 (1976).
[28] J. W. Farmer and Z. Su, Phys. Rev. Lett. **71**, 2979 (1993).
[29] J. W. Farmer and Z. Su, Phys. Rev. Lett. **73**, 367 (1994).
[30] G. Schumm, W. B. Jackson, and R. A. Street, Phys. Rev. B **48**, 14 198 (1993).